

We are IntechOpen, the world's leading publisher of Open Access books Built by scientists, for scientists

6,900

Open access books available

185,000

International authors and editors

200M

Downloads

Our authors are among the

154

Countries delivered to

TOP 1%

most cited scientists

12.2%

Contributors from top 500 universities



WEB OF SCIENCE™

Selection of our books indexed in the Book Citation Index
in Web of Science™ Core Collection (BKCI)

Interested in publishing with us?
Contact book.department@intechopen.com

Numbers displayed above are based on latest data collected.
For more information visit www.intechopen.com



Syntheses and X-Ray Crystal Structures of Magnesium-Substituted Polyoxometalates

Chika Nozaki Kato, Nami Ukai, Daisuke Miyamae,
Shunya Arata, Toshifumi Kashiwagi,
Masaru Nagami, Toshiya Mori, Yusuke Kataoka,
Yasutaka Kitagawa and Hidemitsu Uno

Additional information is available at the end of the chapter

<http://dx.doi.org/10.5772/59598>

1. Introduction

Polyoxometalates have attracted much attention in the fields of catalytic chemistry, surface science, and materials science because their acidity, redox property, and solubility in various media can be controlled at molecular levels [1 – 3]. In particular, coordination of metal ions and organometallics to the vacant site(s) of lacunary polyoxometalates is one of the powerful techniques to construct effective and well-defined metal centers. Among the various metals and their derivatives that can be coordinated to the vacant site(s) of lacunary polyoxometalates, magnesium and magnesium derivatives are intriguing because of their efficient properties as catalysts, reagents for organic syntheses, pharmaceutical compounds, and so on [4, 5]. However, magnesium-coordinated polyoxometalates (characterized by X-ray crystallography) are still one of the least reported compounds: Examples that have been reported include $\text{Mg}_8\text{SiW}_9\text{O}_{37} \cdot 24.5\text{H}_2\text{O}$ [6], $\text{Mg}_8\text{SiW}_9\text{O}_{37} \cdot 12\text{H}_2\text{O}$ [6], and $\text{Mg}_7(\text{MgW}_{12}\text{O}_{42})(\text{OH})_4(\text{H}_2\text{O})_8$ [7].

In this study, we first report the syntheses and molecular structures of cesium and tetra-*n*-butylammonium salts of α -Keggin-type mono-magnesium-substituted polyoxotungstate, i.e., $\text{Cs}_{5.25}\text{H}_{1.75}[\alpha\text{-PW}_{11}\text{MgO}_{40}] \cdot 6\text{H}_2\text{O}$ and $[(n\text{-C}_4\text{H}_9)_4\text{N}]_{4.25}\text{H}_{2.75}[\alpha\text{-PW}_{11}\text{MgO}_{40}] \cdot \text{H}_2\text{O} \cdot \text{CH}_3\text{CN}$, and potassium and dimethylammonium salts of α -Dawson-type mono-magnesium-substituted polyoxotungstate, i.e., $\text{K}_8\text{H}_2[\alpha_2\text{-P}_2\text{W}_{17}\text{MgO}_{62}] \cdot 15\text{H}_2\text{O}$ and $[(\text{CH}_3)_2\text{NH}_2]_{7.5}\text{H}_{2.5}[\alpha_2\text{-P}_2\text{W}_{17}\text{MgO}_{62}] \cdot 6\text{H}_2\text{O}$; these salts were characterized via X-ray crystallography, elemental

analysis, thermogravimetric/differential thermal analysis, Fourier–transform infrared spectroscopy, solution nuclear magnetic resonance spectroscopies, and density-functional-theory (DFT) calculations. The X-ray crystallography results for $\text{Cs}_{5.25}\text{H}_{1.75}[\alpha\text{-PW}_{11}\text{MgO}_{40}] \cdot 6\text{H}_2\text{O}$, $[(n\text{-C}_4\text{H}_9)_4\text{N}]_{4.25}\text{H}_{2.75}[\alpha\text{-PW}_{11}\text{MgO}_{40}] \cdot \text{H}_2\text{O}$, and $[(\text{CH}_3)_2\text{NH}_2]_{7.5}\text{H}_{2.5}[\alpha_2\text{-P}_2\text{W}_{17}\text{MgO}_{62}] \cdot 6\text{H}_2\text{O}$ showed that the mono-magnesium–substituted sites in the α -Keggin and α -Dawson structures could not be identified because of the high symmetry of the compounds, as has been observed for mono-metal–substituted polyoxometalates; however, the bonding modes (i.e., bond lengths and angles) were significantly influenced by the insertion of magnesium ions into the vacant sites. The DFT calculation results also showed that coordination of a hydroxyl group and water molecule to the mono-magnesium–substituted site distorted the molecular structures.

2. Experimental section

2.1. Materials

$\text{K}_7[\alpha\text{-PW}_{11}\text{O}_{39}] \cdot x\text{H}_2\text{O}$ ($x = 16$ and 20) [8] and $\text{K}_{10}[\alpha_2\text{-P}_2\text{W}_{17}\text{O}_{61}] \cdot 14\text{H}_2\text{O}$ [9] were prepared as described in the literature. The number of solvated water molecules was determined by thermogravimetric/differential thermal analyses. All the reagents and solvents were obtained and used as received from commercial sources.

2.2. Instrumentation/analytical procedures

Elemental analyses were carried out by Mikroanalytisches Labor Pascher (Remagen, Germany). Prior to analysis, the samples were dried overnight at room temperature under pressures of 10^{-3} – 10^{-4} Torr. Infrared spectra of the solid samples were recorded on a Perkin Elmer Spectrum100 FT-IR spectrometer in KBr disks at around 25 °C in air. Infrared spectra of the liquid samples were recorded on a Perkin Elmer Frontier FT-IR spectrometer attached to a Universal ATR sampling accessory at around 25 °C in air. Thermogravimetric (TG) and differential thermal analyses (DTA) data were obtained using Rigaku Thermo Plus 2 TG/DTA TG 8120 and Rigaku Thermo Plus EVO2 TG/DTA 81205Z instruments and were performed in air while constantly increasing the temperature from 20 to 500 °C at rates of 1 and 4 °C/min. ^1H (600.17 MHz) and $^{31}\text{P}\{-^1\text{H}\}$ (242.95 MHz) nuclear magnetic resonance (NMR) spectra were recorded in tubes (outer diameter: 5 mm) on a JEOL ECA-600 NMR spectrometer (Shizuoka University). ^1H NMR spectra were measured in dimethylsulfoxide- d_6 and referenced to tetramethylsilane (TMS). Chemical shifts were reported as positive for resonances downfield of TMS (δ 0). ^{31}P NMR spectra were referenced to an external standard of 85% H_3PO_4 in a sealed capillary. Negative chemical shifts were reported on the δ scale for resonances upfield of H_3PO_4 (δ 0). ^{183}W NMR (25.00 MHz) spectra were recorded in tubes (outer diameter: 10 mm) on a JEOL ECA-600 NMR spectrometer (Kyushu University). The ^{183}W NMR spectrum measured in 2.0 mM $\text{Mg}(\text{NO}_3)_2\text{-D}_2\text{O}$ was referenced to an external standard of saturated $\text{Na}_2\text{WO}_4\text{-D}_2\text{O}$ solution (substitution method). Chemical shifts were reported as negative for resonances upfield of Na_2WO_4 (δ 0).

2.3. Synthesis of $\text{Cs}_{5.25}\text{H}_{1.75}[\alpha\text{-PW}_{11}\text{MgO}_{40}] \cdot 6\text{H}_2\text{O}$

Solid $\text{K}_7[\alpha\text{-PW}_{11}\text{O}_{39}] \cdot 20\text{H}_2\text{O}$ (1.01 g; 0.31 mmol) was added to a solution of $\text{MgBr}_2 \cdot 6\text{H}_2\text{O}$ (0.18 g; 0.62 mmol) in 10 mL of water. After stirring for 10 min at 75 °C, solid CsCl (1.02 g; 6.06 mmol) was added to the solution, which was then stirred at 25 °C for 15 min. The resultant white precipitate was collected using a membrane filter (JG 0.2 μm). At this stage, 0.927 g of crude product was obtained. For purification, the crude product (0.927 g) was dissolved in 7 mL of a 3.3 mM solution of MgBr_2 at 75 °C; the resulting solution was filtered through a folded filter paper (Whatman No. 5). After the product was left standing for a day at 25 °C, colorless crystals formed. The obtained crystals weighed 0.384 g (the yield calculated via $[\text{mol of } \text{Cs}_{5.25}\text{H}_{1.75}[\alpha\text{-PW}_{11}\text{MgO}_{40}] \cdot 6\text{H}_2\text{O}] / [\text{mol of } \text{K}_7[\alpha\text{-PW}_{11}\text{O}_{39}] \cdot 20\text{H}_2\text{O}] \times 100\%$ was 35.7%). The elemental analysis results were as follows: H, ≤ 0.1 ; Cs, 20.5; Mg, 0.65; P, 0.87; W, 58.9; Br, 0.01%. The calculated values for $\text{Cs}_{5.25}\text{H}_{1.75}[\alpha\text{-PW}_{11}\text{MgO}_{40}] = \text{H}_{1.75}\text{Mg}_1\text{Cs}_{5.25}\text{O}_{40}\text{P}_1\text{W}_{11}$ were as follows: H, 0.05; Cs, 20.42; Mg, 0.71; P, 0.91; W, 59.18; Br, 0%. A weight loss of 3.03% was observed in the product during overnight drying at room temperature at 10^{-3} – 10^{-4} Torr before the analysis, which suggested that the complex contained six adsorbed water molecules (3.07%). TG/DTA obtained at a heating rate of 4 °C/min under atmospheric conditions showed a weight loss of 3.0% with an endothermic peak at 242 °C in the temperature range of 25 to 500 °C; our calculations indicated the presence of six water molecules (calcd. 3.07%). The results were as follows: IR spectroscopy (KBr disk): 1081s, 1058s, 961s, 888s, 830m, 808m, 769m, 724m cm^{-1} ; IR spectroscopy (in water): 1079m, 1056s, 1017w, 957s, 898m, 823m, 779w, 724w cm^{-1} ; ^{31}P NMR (27 °C, D_2O): δ –10.81.

2.4. Synthesis of $[(n\text{-C}_4\text{H}_9)_4\text{N}]_{4.25}\text{H}_{2.75}[\alpha\text{-PW}_{11}\text{MgO}_{40}] \cdot \text{H}_2\text{O} \cdot \text{CH}_3\text{CN}$

The tetra-*n*-butylammonium salt of $[\alpha\text{-PW}_{11}\text{MgO}_{40}]^{7-}$ was obtained from the reaction of $\text{K}_7[\alpha\text{-PW}_{11}\text{O}_{39}] \cdot 16\text{H}_2\text{O}$ (2.00 g; 0.62 mmol) with $\text{MgBr}_2 \cdot 6\text{H}_2\text{O}$ (0.19 g, 0.65 mmol) in 250 mL of water at 70 °C. After stirring for 1 h at 70 °C, solid $[(\text{CH}_3)_4\text{N}]\text{Br}$ (4.75 g; 30.8 mmol) was added to the solution, which was then stirred at 25 °C for 4 d. The resultant white precipitate was collected using a membrane filter (JG 0.2 μm). The white precipitate (1.708 g) was dissolved in water (350 mL) at 80 °C, $[(n\text{-C}_4\text{H}_9)_4\text{N}]\text{Br}$ (16.99 g; 52.7 mmol) was added to the colorless clear solution, and the solution was stirred at 80 °C for 1 h. The resultant white precipitate was collected on a glass frit (G4). At this stage, 1.862 g of the crude product was obtained. The crude product (1.862 g) was dissolved in acetonitrile (5.5 mL). After filtration through a folded filter paper (Whatman No. 5), colorless crystals were obtained by vapor diffusion from methanol at ~25 °C for one week. The obtained crystals weighed 0.765 g (the yield calculated from $[\text{mol of } [(n\text{-C}_4\text{H}_9)_4\text{N}]_{4.25}\text{H}_{2.75}[\alpha\text{-PW}_{11}\text{MgO}_{40}] \cdot \text{H}_2\text{O} \cdot \text{CH}_3\text{CN}] / [\text{mol of } \text{K}_7[\alpha\text{-PW}_{11}\text{O}_{39}] \cdot 16\text{H}_2\text{O}] \times 100\%$ was 32.5%). The elemental analysis results were as follows: C, 21.5; H, 4.08; N, 1.72; P, 0.83; Mg, 0.63; W, 54.0; K, <0.03%. The calculated values for $[(n\text{-C}_4\text{H}_9)_4\text{N}]_{4.25}\text{H}_{2.75}[\alpha\text{-PW}_{11}\text{MgO}_{40}] \cdot \text{H}_2\text{O} = \text{C}_{68}\text{H}_{157.75}\text{Mg}_1\text{N}_{4.25}\text{O}_{41}\text{P}_1\text{W}_{11}$ were as follows: C, 21.67; H, 4.22; N, 1.58; P, 0.82; Mg, 0.64; W, 53.66; K, 0%. A weight loss of 1.44% from the product was observed during overnight drying at room temperature at 10^{-3} – 10^{-4} Torr before the analysis, which suggested the presence of a weakly solvated or adsorbed acetonitrile molecule (1.08%); this was also supported by the presence of a signal at 2.10 ppm in the ^1H NMR spectrum (in $\text{DMSO}-d_6$) of the sample after drying overnight, which was due to an acetonitrile molecule. TG/DTA results obtained under

atmospheric conditions at a rate of 4 °C/min showed a weight loss of 27.46% with an endothermic peak at 312.2 °C and an exothermic peak at 412.7 °C in the temperature range of 25 to 500 °C; our calculations indicated the presence of 4.25[(C₄H₉)₄N]⁺ ions, a water molecule, and an acetonitrile molecule (calcd. 28.6%). The results were as follows: IR spectroscopy (KBr disk): 1081m, 1060s, 957s, 891s, 819s, 734s cm⁻¹; IR spectroscopy (in acetonitrile): 1082m, 1059s, 955s, 889s, 811s, 733s cm⁻¹; ³¹P NMR (20.5 °C, acetonitrile-*d*₃): δ -10.26.

2.5. Synthesis of K₈H₂[α₂-P₂W₁₇MgO₆₂]·15H₂O

Solid K₁₀[α₂-P₂W₁₇O₆₁]·14H₂O (2.00 g; 0.42 mmol) was added to a solution of Mg(NO₃)₂·6H₂O (0.32 g; 1.25 mmol) in 50 mL of water. After stirring for 2 h at 25 °C, solid KCl (1.57 g; 21.1 mmol) was added to the solution. The resultant white precipitate was collected using a glass frit (G3) and washed with methanol. At this stage, 1.730 g of a crude product was obtained. For purification, the crude product (1.730 g) was dissolved in 17 mL of a 2.0 mM Mg(NO₃)₂ aqueous solution; the resulting solution was filtered through a folded filter paper (Whatman No. 5). After standing in a refrigerator overnight, white crystals formed, which were collected using a membrane filter (JG 0.2 μm) and yielded 0.693 g of product. The percent yield calculated using [mol of K₈H₂[α₂-P₂W₁₇MgO₆₂]·15H₂O]/[mol of K₁₀[α₂-P₂W₁₇O₆₁]·14H₂O] × 100% was 34.8 %. The elemental analysis results were as follows: H, <0.1; K, 7.17; Mg, 0.52; P, 1.34; W, 68.6; N, <0.1%; the calculated values for K₈H₂[α₂-P₂W₁₇MgO₆₂]·xH₂O (x = 1) = H₄K₈Mg₁O₆₃P₂W₁₇ were H, 0.09; K, 6.90; Mg, 0.54; P, 1.37; W, 68.89; N, 0%. A weight loss of 5.30% was observed during overnight drying at room temperature at 10⁻³–10⁻⁴ Torr before analysis, suggesting the presence of 14 weakly solvated or adsorbed water molecules (5.27%). TG/DTA results obtained at a heating rate of 4 °C/min under atmospheric conditions showed a weight loss of 5.62% below 500 °C with an endothermic point at 101.4 °C; calculations showed that 5.64% corresponded to 15 water molecules. The results were as follows: IR spectroscopy (KBr disk): 1084s, 1063m, 1015m, 945s, 920s, 892sh, 823s, 786s, 736s cm⁻¹; IR spectroscopy (in water): 1086s, 1064m, 1015w, 946s, 914s, 811s, 788s, 724m cm⁻¹; ³¹P NMR (D₂O, 23.9 °C): δ -7.77, -13.77. ¹⁸³W NMR (2.0 mM Mg(NO₃)₂-D₂O, 40 °C): δ -57.04, -80.87, -131.47, -176.59, -181.67, -201.40, -207.65, -208.63, -230.51.

2.6. Synthesis of [(CH₃)₂NH₂]_{7.5}H_{2.5}[α₂-P₂W₁₇MgO₆₂]·6H₂O

The dimethylammonium salt of [α₂-P₂W₁₇MgO₆₂]¹⁰⁻ was obtained via the reaction of K₁₀[α₂-P₂W₁₇O₆₁]·14H₂O (2.00 g; 0.42 mmol) with Mg(NO₃)₂·6H₂O (0.11g; 0.43 mmol) in 50 mL of water. After stirring for 1 h at 25 °C, solid (CH₃)₂NHHCl (3.44 g; 42.2mmol) was added to the solution. The resultant white precipitate was collected using a glass frit (G4). At this stage, 1.363 g of the crude product was obtained. For purification, the crude product (1.363 g) was dissolved in 32 mL of water. After filtration through a folded filter paper (Whatman No. 5), colorless crystals were obtained by vapor diffusion from ethanol at 25 °C for 4 d. The obtained crystals weighed 0.740 g (the yield calculated from [mol of [(CH₃)₂NH₂]_{7.5}H_{2.5}[α₂-P₂W₁₇MgO₆₂]·6H₂O]/[mol of K₁₀[α₂-P₂W₁₇O₆₁]·14H₂O] × 100% was 38.1%). The elemental analysis results were as follows: C, 3.72; H, 1.42; N, 2.50; Mg, 0.42; P, 1.34; W, 68.0; K, <0.1%; the calculated values for [(CH₃)₂NH₂]_{7.5}H_{2.5}[α₂-P₂W₁₇MgO₆₂]·xH₂O (x = 3) = C₁₅H_{68.5}Mg₁N_{7.5}O₆₅P₂W₁₇ were C, 3.91; H, 1.50; N, 2.28; Mg,

0.53; P, 1.35; W, 67.86; K, 0%. A weight loss of 1.30% was observed during overnight drying at room temperature at 10^{-3} – 10^{-4} Torr before analysis, suggesting the presence of three weakly solvated or adsorbed water molecules (1.16%). TG/DTA results obtained at a rate of 1 °C/min under atmospheric conditions showed weight losses of 2.33% and 7.42% without clear endothermic and exothermic points in the temperature ranges of 25 to 200 °C and 200 to 500 °C, respectively; calculations showed that 2.32% and 7.42% corresponded to six water molecules and 7.5 dimethylammonium ions, respectively. The results were as follows: IR spectroscopy (KBr disk): 1087s, 1065m, 1018m, 948s, 919s, 891s, 805s, 777s, 717s cm^{-1} ; IR spectroscopy (in water): 1086s, 1065m, 1020w, 945s, 913s, 808s, 790s, 723m cm^{-1} ; ^{31}P NMR (D_2O , 21.7 °C): δ -7.73, -13.74.

2.7. X-Ray crystallography

A colorless prism crystal of $\text{Cs}_{5.25}\text{H}_{1.75}[\alpha\text{-PW}_{11}\text{MgO}_{40}] \cdot 6\text{H}_2\text{O}$ (0.090 × 0.070 × 0.060 mm), colorless platelet crystal of $[(n\text{-C}_4\text{H}_9)_4\text{N}]_{4.25}\text{H}_{2.75}[\alpha\text{-PW}_{11}\text{MgO}_{40}] \cdot \text{H}_2\text{O} \cdot \text{CH}_3\text{CN}$ (0.200 × 0.100 × 0.020 mm), and colorless block crystal of $[(\text{CH}_3)_2\text{NH}_2]_{7.5}\text{H}_{2.5}[\alpha_2\text{-P}_2\text{W}_{17}\text{MgO}_{62}] \cdot 6\text{H}_2\text{O}$ (0.200 × 0.100 × 0.100 mm) were mounted on a loop or MicroMount. The measurements for the cesium and tetra-*n*-butylammonium salts of α -Keggin mono-magnesium-substituted polyoxotungstate were obtained using a Rigaku VariMax with a Saturn diffractometer using multi-layer mirror-monochromated Mo K α radiation ($\lambda = 0.71075$ Å) at 100 ± 1 K. The measurement for the dimethylammonium salt of α -Dawson mono-magnesium-substituted polyoxotungstate was carried out using a Rigaku VariMax with an XtaLAB P200 diffractometer using multi-layer mirror-monochromated Mo K α radiation ($\lambda = 0.71075$ Å) at 153 ± 1 K. Data were collected and processed using CrystalClear, CrystalClear-SM Expert for Windows, and structural analysis was performed using CrystalStructure for Windows. The structure was solved by SHELXS-97, SHELXS-2013, and SIR-2004 (direct methods) and refined by SHELXL-97 and SHELXL2013 [10, 11]. In these magnesium compounds, a magnesium atom was disordered over ten and twelve tungsten atoms in $[\alpha\text{-PW}_{11}\text{MgO}_{40}]^{7-}$, and six tungsten atoms at B-sites (cap units) in $[\alpha\text{-PW}_{17}\text{MgO}_{62}]^{10-}$. The occupancies for the magnesium and tungsten atoms were fixed at 1/10 and 9/10, 1/12 and 11/12, and 1/6 and 5/6, respectively. For $\text{Cs}_{5.25}\text{H}_{1.75}[\alpha\text{-PW}_{11}\text{MgO}_{40}] \cdot 6\text{H}_2\text{O}$, 5.25 cesium ions were disordered at Cs(1) and Cs(2) and the water molecules were disordered. For the structural analysis of $[(\text{CH}_3)_2\text{NH}_2]_{7.5}\text{H}_{2.5}[\alpha_2\text{-P}_2\text{W}_{17}\text{MgO}_{62}] \cdot 6\text{H}_2\text{O}$, the chemical formula of $[(\text{CH}_3)_2\text{NH}_2]_{7.5}\text{H}_{2.5}[\alpha_2\text{-P}_2\text{W}_{17}\text{MgO}_{62}] \cdot 3\text{H}_2\text{O}$ was used, and the water molecules were also disordered. With regard to $[(n\text{-C}_4\text{H}_9)_4\text{N}]_{4.25}\text{H}_{2.75}[\alpha\text{-PW}_{11}\text{MgO}_{40}] \cdot \text{H}_2\text{O} \cdot \text{CH}_3\text{CN}$, tetra-*n*-butylammonium ions, water molecules, and acetonitrile molecules could not be modeled because of disorder of the atoms. Accordingly, the residual electron density was removed using the SQUEEZE routine in PLATON [12]. Disordered counter-cations and solvated molecules are common in polyoxometalate chemistry [13 – 16].

2.8. Crystal data for $\text{Cs}_{5.25}\text{H}_{1.75}[\alpha\text{-PW}_{11}\text{MgO}_{40}] \cdot 6\text{H}_2\text{O}$

$\text{H}_{13.75}\text{Cs}_{5.25}\text{MgO}_{46}\text{PW}_{11}$; $M = 3525.27$, tetragonal, space group: $P4_2/ncm$ (#138), $a = 20.859(4)$ Å, $c = 10.387(2)$ Å, $V = 4520(2)$ Å³, $Z = 4$, $D_c = 5.181$ g/cm³, $\mu(\text{Mo K}\alpha) = 321.99$ cm⁻¹, $R_1 = 0.0508$ [$I > 2\sigma(I)$], $wR_2 = 0.1070$ (for all data). GOF = 1.248 [52491 total reflections and 2703 unique reflections where $I > 2\sigma(I)$]. CCDC No. 1020993

2.9. Crystal data for $[(n\text{-C}_4\text{H}_9)_4\text{N}]_{4.25}\text{H}_{2.75}[\alpha\text{-PW}_{11}\text{MgO}_{40}]\cdot\text{H}_2\text{O}\cdot\text{CH}_3\text{CN}$

$\text{C}_{70}\text{H}_{160.75}\text{MgN}_{5.25}\text{O}_{41}\text{PW}_{11}$; $M = 3809.93$, *cubic*, space group: $Im\text{-}3m$ (#229), $a = 17.650(6)$ Å, $V = 5498(3)$ Å³, $Z = 2$, $D_c = 2.301$ g/cm³, $\mu(\text{Mo K}\alpha) = 115.627$ cm⁻¹, $R_1 = 0.0578$ [$I > 2\sigma(I)$], $wR_2 = 0.1312$ (for all data). GOF = 1.181 (44531 total reflections, 653 unique reflections where $I > 2\sigma(I)$). CCDC No. 1020994

2.10. Crystal data for $[(\text{CH}_3)_2\text{NH}_2]_{7.5}\text{H}_{2.5}[\alpha_2\text{-P}_2\text{W}_{17}\text{MgO}_{62}]\cdot 3\text{H}_2\text{O}$

$\text{C}_{15}\text{H}_{68.50}\text{MgN}_{7.50}\text{O}_{65}\text{P}_2\text{W}_{17}$; $M = 4605.92$, *orthorhombic*, space group: $Pnma$ (#62), $a = 27.7901(12)$ Å, $b = 20.4263(9)$ Å, $c = 15.0638(6)$ Å, $V = 8550.9(7)$ Å³, $Z = 4$, $D_c = 3.577$ g/cm³, $\mu(\text{Mo K}\alpha) = 229.323$ cm⁻¹, $R_1 = 0.0685$ [$I > 2\sigma(I)$], $wR_2 = 0.1980$ (for all data). GOF = 1.096 (95493 total reflections, 12764 unique reflections where $I > 2\sigma(I)$). CCDC No. 1020995

2.11. Computational details

The optimal geometries of $[\alpha\text{-PW}_{11}\{\text{Mg}(\text{OH})\}\text{O}_{39}]^{6-}$ and $[\alpha\text{-PW}_{11}\{\text{Mg}(\text{OH}_2)\}\text{O}_{39}]^{5-}$ were computed using a DFT method. First, we optimized the molecular geometries and then applied single-point calculations with larger basis sets. All calculations were performed using a spin-restricted B3LYP method with the Gaussian09 program package [17]. The solvent effect of acetonitrile was considered using the polarizable continuum model. The basis sets used for geometry optimization were LANL2DZ for the W atoms, 6-31+G* for the P atoms, and 6-31G* for the H, O, and Mg atoms. LANL2DZ and 6-31+G* were used for the W and other atoms, respectively, for the single-point calculations. Geometry optimization was started using the X-ray structure of $[\alpha\text{-PW}_{12}\text{O}_{40}]^{3-}$ as the initial geometry, and was performed in acetonitrile. The optimized geometries were confirmed to be true minima by frequency analyses. All atomic charges used in this text were obtained from Mulliken population analysis. Zero-point energy-corrected total energies were used to consider the structural stabilities of $[\alpha\text{-PW}_{11}\{\text{Mg}(\text{OH})\}\text{O}_{39}]^{6-}$ and $[\alpha\text{-PW}_{11}\{\text{Mg}(\text{OH}_2)\}\text{O}_{39}]^{5-}$.

3. Results and discussion

3.1. Syntheses and molecular structures of cesium and tetra-*n*-butylammonium salts of α -Keggin mono-magnesium-substituted polyoxotungstate $\text{Cs}_{5.25}\text{H}_{1.75}[\alpha\text{-PW}_{11}\text{MgO}_{40}]\cdot 6\text{H}_2\text{O}$ and $[(n\text{-C}_4\text{H}_9)_4\text{N}]_{4.25}\text{H}_{2.75}[\alpha\text{-PW}_{11}\text{MgO}_{40}]\cdot\text{H}_2\text{O}\cdot\text{CH}_3\text{CN}$

The cesium salt of $[\alpha\text{-PW}_{11}\text{MgO}_{40}]^{7-}$ was formed by the direct reaction of magnesium bromide with $[\alpha\text{-PW}_{11}\text{O}_{39}]^{7-}$ (at a $\text{Mg}^{2+}/[\alpha\text{-PW}_{11}\text{O}_{39}]^{7-}$ ratio of ~ 2.0) in aqueous solution, followed by the addition of excess cesium chloride. The pure cesium salt was not obtained by a stoichiometric reaction of Mg^{2+} with $[\alpha\text{-PW}_{11}\text{O}_{39}]^{7-}$ in aqueous solution. Crystallization was performed via slow-evaporation from a 3.3 mM MgBr_2 solution at 70 °C. Here, single crystals suitable for X-ray crystallography could not be obtained in water because a mono-lacunary polyoxoanion formed upon the removal of magnesium ions from $[\alpha\text{-PW}_{11}\text{MgO}_{40}]^{7-}$ in water at around 70 °C. In contrast, the tetra-*n*-butylammonium salt of $[\alpha\text{-PW}_{11}\text{MgO}_{40}]^{7-}$ was formed by a stoichiometric reaction of magnesium bromide with $[\alpha\text{-PW}_{11}\text{O}_{39}]^{7-}$ in aqueous solution, followed by the

addition of excess tetra-*n*-butylammonium bromide. Crystallization was performed by vapor diffusion from acetonitrile/methanol at ~25 °C.

Samples for the elemental analyses were dried overnight at room temperature under a vacuum of 10^{-3} – 10^{-4} Torr. The elemental analysis results for H, Cs, Mg, P, and W were in good agreement with the calculated values for the formula of $\text{Cs}_{5.25}\text{H}_{1.75}[\alpha\text{-PW}_{11}\text{MgO}_{40}]$. Br analysis revealed no contamination of bromide ions from MgBr_2 . The weight loss observed during the course of drying before the analysis was 3.03% for $\text{Cs}_{5.25}\text{H}_{1.75}[\alpha\text{-PW}_{11}\text{MgO}_{40}] \cdot 6\text{H}_2\text{O}$; this corresponded to six weakly solvated or adsorbed water molecules. TG/DTA measurements also showed a weight loss of 3.1% in the temperature range of 25 to 500 °C, which corresponded to six water molecules. For the tetra-*n*-butylammonium salt, the elemental analysis results for C, H, N, P, Mg, and W were in good agreement with the calculated values for the formula of $[(n\text{-C}_4\text{H}_9)_4\text{N}]_{4.25}\text{H}_{2.75}[\alpha\text{-PW}_{11}\text{MgO}_{40}] \cdot \text{H}_2\text{O}$. K analysis revealed no contamination of potassium ions from $\text{K}_7[\alpha\text{-PW}_{11}\text{O}_{39}]$. The weight loss observed during the course of drying before the analysis was 1.44% for $[(n\text{-C}_4\text{H}_9)_4\text{N}]_{4.25}\text{H}_{2.75}[\alpha\text{-PW}_{11}\text{MgO}_{40}] \cdot \text{H}_2\text{O} \cdot \text{CH}_3\text{CN}$; this corresponded to one weakly solvated or adsorbed acetonitrile molecule. The ^1H NMR spectrum in $\text{DMSO-}d_6$ also showed the presence of an acetonitrile molecule in the sample after drying under vacuum overnight. TG/DTA measurements showed a weight loss of 27.46% in the temperature range of 25 to 500 °C, which corresponded to 4.25 $[(\text{C}_4\text{H}_9)_4\text{N}]^+$ ions, a water molecule, and an acetonitrile molecule.

The molecular structures of cesium and tetra-*n*-butylammonium salts of $[\alpha\text{-PW}_{11}\text{MgO}_{40}]^{7-}$ as determined by X-ray crystallography, are shown in Figs. 1 and 2. The lengths of the bonds involving oxygen atoms in the central PO_4 tetrahedron (O_a), bridging oxygen atoms between corner-sharing MO_6 ($\text{M} = \text{W}$ and Mg) octahedra (O_c), bridging oxygen atoms between edge-sharing MO_6 octahedra (O_e), and terminal oxygen atoms (O_t) are summarized in Table 1. The molecular structures of these magnesium compounds were identical to that of a monomeric, α -Keggin polyoxotungstate $[\alpha\text{-PW}_{12}\text{O}_{40}]^{3-}$ [18, 19]. Due to the high-symmetry space groups of the structures, the ten or eleven tungsten(VI) atoms were disordered and the mono-magnesium-substituted site was not identified, as previously reported for $[\alpha\text{-PW}_{11}\{\text{Al}(\text{OH}_2)\}\text{O}_{39}]^{4-}$ [20]. However, it was clear that the average bond lengths of $\text{W}(\text{Mg})\text{-O}_a$ in $\text{Cs}_{5.25}\text{H}_{1.75}[\alpha\text{-PW}_{11}\text{MgO}_{40}] \cdot 6\text{H}_2\text{O}$ (2.478 Å) and $[(n\text{-C}_4\text{H}_9)_4\text{N}]_{4.25}\text{H}_{2.75}[\alpha\text{-PW}_{11}\text{MgO}_{40}] \cdot \text{H}_2\text{O} \cdot \text{CH}_3\text{CN}$ (2.483 Å) were longer than those of $[\text{CH}_3\text{NH}_3]_3[\text{PW}_{12}\text{O}_{40}] \cdot 2\text{H}_2\text{O}$ (2.4398 Å), $[(\text{CH}_3)_2\text{NH}_2]_3[\text{PW}_{12}\text{O}_{40}]$ (2.4430 Å), and $[(\text{CH}_3)_3\text{NH}]_3[\text{PW}_{12}\text{O}_{40}]$ (2.4313 Å) [19] (Table 1); this suggested that the magnesium ion was coordinated to the mono-lacunary Keggin-type polyoxotungstate.

Although a hydroxyl group and/or water molecule should be coordinated to the magnesium site in $[\alpha\text{-PW}_{11}\text{MgO}_{40}]^{7-}$, it could not be identified by X-ray crystallography. On the basis of the Cs analysis results, $\text{Cs}_{5.25}\text{H}_{1.75}[\alpha\text{-PW}_{11}\text{MgO}_{40}] \cdot 6\text{H}_2\text{O}$ should contain species with hydroxyl groups in at least 25% of the molecules. To investigate the coordination spheres around the mono-magnesium-substituted sites containing a hydroxyl group and water molecule, optimized geometries of $[\alpha\text{-PW}_{11}\{\text{Mg}(\text{OH})\}\text{O}_{39}]^{6-}$ and $[\alpha\text{-PW}_{11}\{\text{Mg}(\text{OH}_2)\}\text{O}_{39}]^{5-}$ were computed by means of a DFT method, as shown in Fig. 3. The bond-length ranges, mean bond distances, and Mulliken charges for DFT-optimized $[\alpha\text{-PW}_{11}\{\text{Mg}(\text{OH})\}\text{O}_{39}]^{6-}$ and $[\alpha\text{-PW}_{11}\{\text{Mg}(\text{OH}_2)\}\text{O}_{39}]^{5-}$ are summarized in Tables 2 and 3. As shown in Fig. 3, the ligands coordinated to the mono-magnesium-substituted site caused remarkable distortion of the α -Keggin molecular structure:

The Mg–P distance of $[\alpha\text{-PW}_{11}\{\text{Mg}(\text{OH})\}\text{O}_{39}]^{6-}$ was 3.652 Å, which was longer than that of $[\alpha\text{-PW}_{11}\{\text{Mg}(\text{OH}_2)\}\text{O}_{39}]^{5-}$ (3.330 Å). The charges of all atoms in $[\alpha\text{-PW}_{11}\{\text{Mg}(\text{OH})\}\text{O}_{39}]^{6-}$ and $[\alpha\text{-PW}_{11}\{\text{Mg}(\text{OH}_2)\}\text{O}_{39}]^{5-}$ were also influenced by the ligands, as shown in Table 3.

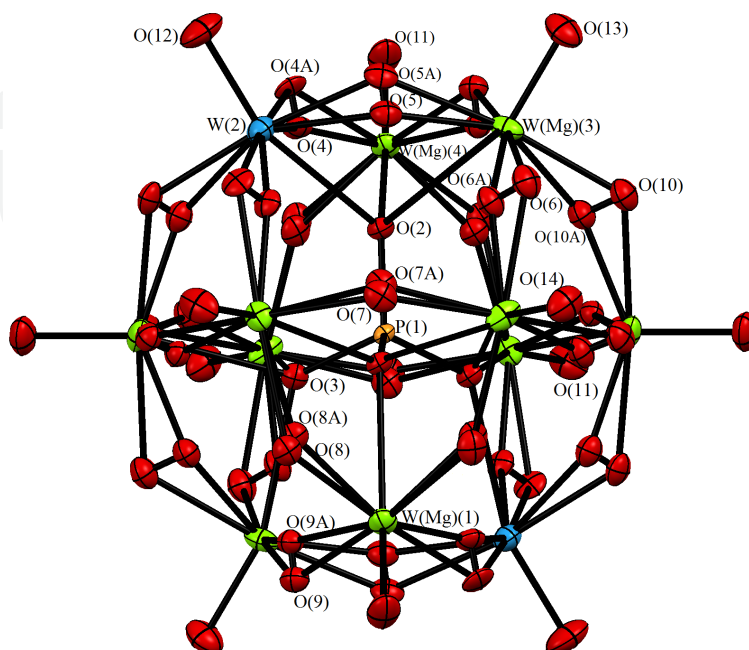


Figure 1. The molecular structure (ORTEP drawing) of $\text{Cs}_{5.25}\text{H}_{1.75}[\alpha\text{-PW}_{11}\text{MgO}_{40}]\cdot 6\text{H}_2\text{O}$. The corner- and edge-sharing oxygen atoms in the α -Keggin structure were disordered. W(2) was clearly identified; however, a magnesium atom was disordered over ten tungsten sites in $[\alpha\text{-PW}_{11}\text{MgO}_{40}]^{7-}$, and the occupancies for the magnesium and tungsten sites were fixed at 1/10 and 9/10 throughout the refinement.

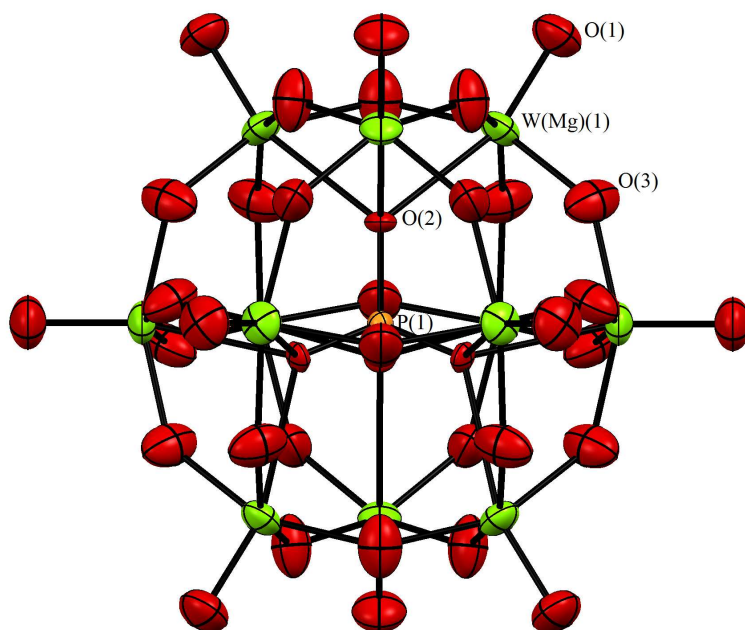


Figure 2. The molecular structure (ORTEP drawing) of $[(n\text{-C}_4\text{H}_9)_4\text{N}]_{4.25}\text{H}_{2.75}[\alpha\text{-PW}_{11}\text{MgO}_{40}]\cdot \text{H}_2\text{O}$. A magnesium atom was disordered over eleven tungsten sites in $[\alpha\text{-PW}_{11}\text{MgO}_{40}]^{7-}$, and the occupancies for the magnesium and tungsten sites were fixed at 1/12 and 11/12 throughout the refinement.

$\text{Cs}_{5.25}\text{H}_{1.75}[\alpha\text{-PW}_{11}\text{MgO}_{40}]\cdot 6\text{H}_2\text{O}$	
W(Mg)-O _a	2.426 – 2.521 (2.478)
W(Mg)-O _c	1.827 – 2.426 (1.945)
W(Mg)-O _e	1.827 – 2.426 (1.945)
W(Mg)-O _t	1.688 – 1.712 (1.696)
W(2)-O _a	2.423
W(2)-O _c	1.859 – 1.979 (1.927)
W(2)-O _e	1.859 – 1.979 (1.927)
W(2)-O _t	1.726
P-O	1.544 – 1.590 (1.562)
$[(n\text{-C}_4\text{H}_9)_4\text{N}]_{4.25}\text{H}_{2.75}[\alpha\text{-PW}_{11}\text{MgO}_{40}]\cdot \text{H}_2\text{O}\cdot \text{CH}_3\text{CN}$	
W(Mg)-O _a	2.483 (2.483)
W(Mg)-O _c	1.894 (1.894)
W(Mg)-O _e	1.894 (1.894)
W(Mg)-O _t	1.703 (1.703)
P-O	1.511 (1.511)

Table 1. Ranges and mean bond distances (Å) of $\text{Cs}_{5.25}\text{H}_{1.75}[\alpha\text{-PW}_{11}\text{MgO}_{40}]\cdot 6\text{H}_2\text{O}$ and $[(n\text{-C}_4\text{H}_9)_4\text{N}]_{4.25}\text{H}_{2.75}[\alpha\text{-PW}_{11}\text{MgO}_{40}]\cdot \text{H}_2\text{O}\cdot \text{CH}_3\text{CN}$. O_a: oxygen atoms belonging to the central PO₄ tetrahedron; O_c: bridging oxygen atoms between corner-sharing MO₆ (M = Mg and W) octahedra; O_e: bridging oxygen atoms between edge-sharing MO₆ octahedra (M = Mg and W); and O_t: terminal oxygen atoms. The mean values are provided in parentheses.

Here, the sum of the zero-point energy-corrected total energies (Hartree) of ($[\alpha\text{-PW}_{11}\{\text{Mg}(\text{OH})\}\text{O}_{39}]^{6-} + \text{H}_3\text{O}^+$) and ($[\alpha\text{-PW}_{11}\{\text{Mg}(\text{OH}_2)\}\text{O}_{39}]^{5-} + \text{H}_2\text{O}$) was -4377.185183 and -4377.287786 , respectively; the thermal energy of ($[\alpha\text{-PW}_{11}\{\text{Mg}(\text{OH}_2)\}\text{O}_{39}]^{5-} + \text{H}_2\text{O}$) calculated on the basis of zero-point energy was 64.4 kcal/mol lower than that of ($[\alpha\text{-PW}_{11}\{\text{Mg}(\text{OH})\}\text{O}_{39}]^{6-} + \text{H}_3\text{O}^+$). Thus, $[\alpha\text{-PW}_{11}\{\text{Mg}(\text{OH}_2)\}\text{O}_{39}]^{5-}$ was more stable than $[\alpha\text{-PW}_{11}\{\text{Mg}(\text{OH})\}\text{O}_{39}]^{6-}$. It was noted that the Mg-O_c and Mg-O_e bond lengths of the optimized $[\alpha\text{-PW}_{11}\{\text{Mg}(\text{OH})\}\text{O}_{39}]^{6-}$ structure were longer than those of $[\alpha\text{-PW}_{11}\{\text{Mg}(\text{OH}_2)\}\text{O}_{39}]^{5-}$, as shown in Table 2. In the X-ray crystal structures of $\text{Cs}_{5.25}\text{H}_{1.75}[\alpha\text{-PW}_{11}\text{MgO}_{40}]\cdot 6\text{H}_2\text{O}$ and $[(n\text{-C}_4\text{H}_9)_4\text{N}]_{4.25}\text{H}_{2.75}[\alpha\text{-PW}_{11}\text{MgO}_{40}]\cdot \text{H}_2\text{O}\cdot \text{CH}_3\text{CN}$, the mean W(Mg)-O_c and W(Mg)-O_e bond lengths of the cesium salt were longer than those of the tetra-*n*-butylammonium salt. The mean P-O bond length of $\text{Cs}_{5.25}\text{H}_{1.75}[\alpha\text{-PW}_{11}\text{MgO}_{40}]\cdot 6\text{H}_2\text{O}$ (1.562 Å) was also longer than that of $[(n\text{-C}_4\text{H}_9)_4\text{N}]_{4.25}\text{H}_{2.75}[\alpha\text{-PW}_{11}\text{MgO}_{40}]\cdot \text{H}_2\text{O}\cdot \text{CH}_3\text{CN}$ (1.511 Å); this was consistent with the DFT calculation results. These results suggested that $\text{Cs}_{5.25}\text{H}_{1.75}[\alpha\text{-PW}_{11}\text{MgO}_{40}]\cdot 6\text{H}_2\text{O}$ contained both $[\alpha\text{-PW}_{11}\{\text{Mg}(\text{OH})\}\text{O}_{39}]^{6-}$ and $[\alpha\text{-PW}_{11}\{\text{Mg}(\text{OH}_2)\}\text{O}_{39}]^{5-}$; in contrast, the molecular structure of $[(n\text{-C}_4\text{H}_9)_4\text{N}]_{4.25}\text{H}_{2.75}[\alpha\text{-PW}_{11}\text{MgO}_{40}]\cdot \text{H}_2\text{O}\cdot \text{CH}_3\text{CN}$ was predominantly $[\alpha\text{-PW}_{11}\{\text{Mg}(\text{OH}_2)\}\text{O}_{39}]^{5-}$.

The ³¹P NMR spectrum in D₂O of $\text{Cs}_{5.25}\text{H}_{1.75}[\alpha\text{-PW}_{11}\text{MgO}_{40}]\cdot 6\text{H}_2\text{O}$ showed a signal at -10.8 ppm that corresponded to the internal phosphorus atom; this demonstrated the high purity of

$\text{Cs}_{5.25}\text{H}_{1.75}[\alpha\text{-PW}_{11}\text{MgO}_{40}] \cdot 6\text{H}_2\text{O}$ in water. However, the presence of polyoxoanions possessing Mg-OH and/or Mg-OH_2 moieties could not be identified by ^{31}P NMR spectroscopy in water. For the ^{31}P NMR spectrum in acetonitrile- d_3 of $[(n\text{-C}_4\text{H}_9)_4\text{N}]_{4.25}\text{H}_{2.75}[\alpha\text{-PW}_{11}\text{MgO}_{40}] \cdot \text{H}_2\text{O} \cdot \text{CH}_3\text{CN}$, a signal was also observed at -10.3 ppm. These signals exhibited a shift from the signals of $\text{K}_7[\alpha\text{-PW}_{11}\text{O}_{39}]$ ($\delta -10.6$) in D_2O and the tetra- n -butylammonium salt of $[\alpha\text{-PW}_{11}\text{O}_{39}]^{7-}$ ($\delta -12.0$) in acetonitrile- d_3 , respectively. This showed that the magnesium ion was inserted into the vacant site.

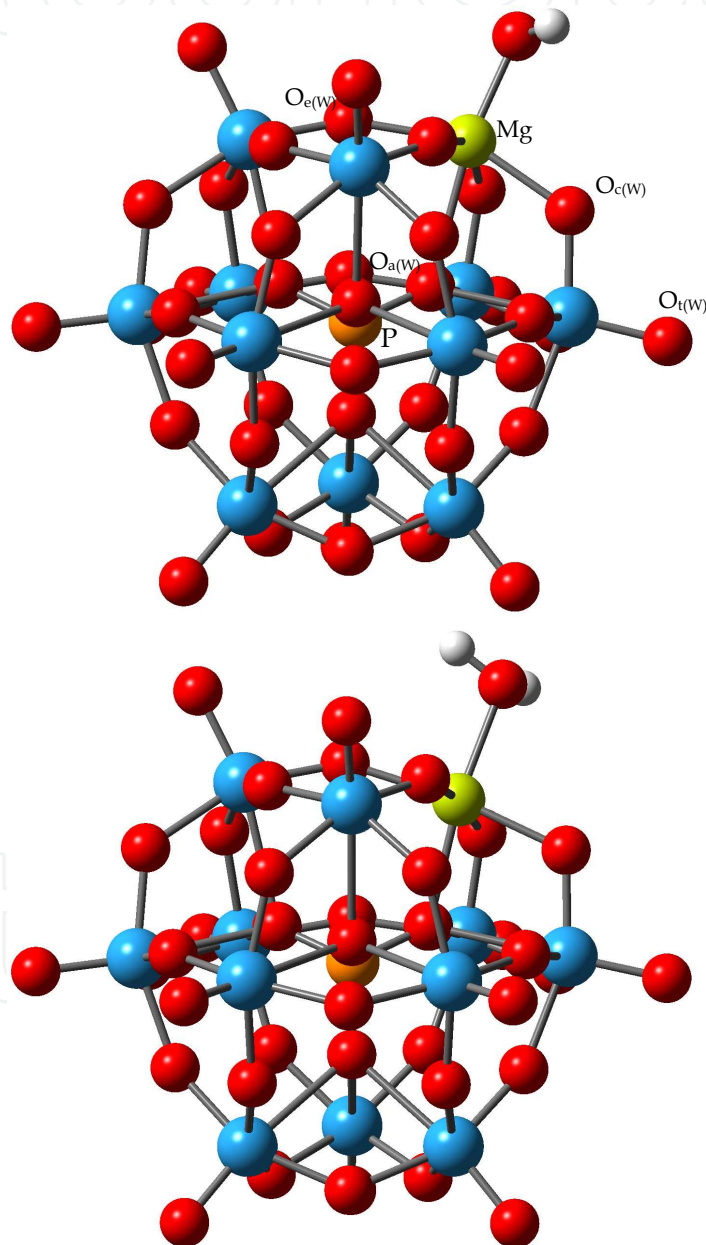


Figure 3. DFT-optimized geometries of $[\alpha\text{-PW}_{11}\{\text{Mg}(\text{OH})\}\text{O}_{39}]^{6-}$ (top) and $[\alpha\text{-PW}_{11}\{\text{Mg}(\text{OH}_2)\}\text{O}_{39}]^{5-}$ (bottom). The phosphorus, oxygen, magnesium, tungsten, and hydrogen atoms are represented by orange, red, green, blue, and white balls, respectively.

	$[\alpha\text{-PW}_{11}\{\text{Mg}(\text{OH})\}\text{O}_{39}]^{6-}$	$[\alpha\text{-PW}_{11}\{\text{Mg}(\text{OH}_2)\}\text{O}_{39}]^{5-}$
W-O _a	2.42491 – 2.50502 (2.45747)	2.43078 – 2.49519 (2.46749)
W-O _c	1.77745 – 2.06287 (1.92795)	1.78987 – 2.04292 (1.92730)
W-O _e	1.77336 – 2.06166 (1.92035)	1.78511 – 2.03477 (1.92000)
W-O _t	1.72294 – 1.73069 (1.72654)	1.72076 – 1.72696 (1.72356)
P-O	1.54748 – 1.56478 (1.55930)	1.55541 – 1.55857 (1.55763)
Mg-O _a	2.52990 (2.52990)	2.18152 (2.18152)
Mg-O _c	2.10554 – 2.11671 (2.11113)	2.04263 – 2.05034 (2.04649)
Mg-O _e	2.08702 – 2.09720 (2.09211)	2.06585 – 2.08177 (2.07381)
Mg-OH/OH ₂	1.93732 (1.93732)	2.12343 (2.12343)

Table 2. Ranges and mean bond distances (Å) of $[\alpha\text{-PW}_{11}\{\text{Mg}(\text{OH})\}\text{O}_{39}]^{6-}$ and $[\alpha\text{-PW}_{11}\{\text{Mg}(\text{OH}_2)\}\text{O}_{39}]^{5-}$ optimized by DFT calculations. The mean values are provided in parentheses.

	$[\alpha\text{-PW}_{11}\{\text{Mg}(\text{OH})\}\text{O}_{39}]^{6-}$	$[\alpha\text{-PW}_{11}\{\text{Mg}(\text{OH}_2)\}\text{O}_{39}]^{5-}$
O _{a(W)}	−0.752 – −0.731 (−0.740)	−0.789 – −0.752 (−0.768)
O _{c(W)}	−1.166 – −0.975 (−1.084)	−1.170 – −1.009 (−1.095)
O _{e(W)}	−1.359 – −1.143 (−1.300)	−1.366 – −1.194 (−1.314)
O _{t(W)}	−0.774 – −0.725 (−0.748)	−0.743 – −0.708 (−0.730)
P	6.849	7.192
W	2.105 – 2.474 (2.304)	2.151 – 2.460 (2.313)
O _{a(Mg)}	−0.489	−0.481
O _{c(Mg)}	−0.694 – −0.680 (−0.687)	−0.749 – −0.690 (−0.720)
O _{e(Mg)}	−0.638 – −0.616 (−0.627)	−0.674 – −0.636 (−0.655)
O _{t(Mg)}	−0.961	−0.844
Mg	−0.253	−0.274
H	0.428	0.556 – 0.564 (0.560)

Table 3. Mulliken charges computed for $[\alpha\text{-PW}_{11}\{\text{Mg}(\text{OH})\}\text{O}_{39}]^{6-}$ and $[\alpha\text{-PW}_{11}\{\text{Mg}(\text{OH}_2)\}\text{O}_{39}]^{5-}$. The mean values are provided in parentheses.

The FT-IR spectra measured as KBr disks of $\text{Cs}_{5.25}\text{H}_{1.75}[\alpha\text{-PW}_{11}\text{MgO}_{40}] \cdot 6\text{H}_2\text{O}$ and $[(n\text{-C}_4\text{H}_9)_4\text{N}]_{4.25}\text{H}_{2.75}[\alpha\text{-PW}_{11}\text{MgO}_{40}] \cdot \text{H}_2\text{O} \cdot \text{CH}_3\text{CN}$ are shown in Fig. 4. These spectra showed bands at 1081, 1058, 961, 888, 830, 808, 769, and 724 cm^{-1} and 1081, 1060, 957, 891, 819, and 734 cm^{-1} , respectively; these bands were different from those of $\text{K}_7[\alpha\text{-PW}_{11}\text{O}_{39}]$ (1086, 1043, 953, 903, 862, 810, and 734 cm^{-1}) [21, 22]. This also supported that the magnesium ion was coordinated to the vacant site in the polyoxometalate.

The spectral pattern of solid $\text{Cs}_{5.25}\text{H}_{1.75}[\alpha\text{-PW}_{11}\text{MgO}_{40}] \cdot 6\text{H}_2\text{O}$ was different from that of solid $[(n\text{-C}_4\text{H}_9)_4\text{N}]_{4.25}\text{H}_{2.75}[\alpha\text{-PW}_{11}\text{MgO}_{40}] \cdot \text{H}_2\text{O} \cdot \text{CH}_3\text{CN}$ even though the counter-ions affected their spectra [21, 22]. As shown in Fig. 5, the FT-IR spectral pattern of solid $[(n\text{-C}_4\text{H}_9)_4\text{N}]_{4.25}\text{H}_{2.75}[\alpha\text{-PW}_{11}\text{MgO}_{40}] \cdot \text{H}_2\text{O} \cdot \text{CH}_3\text{CN}$ was the same as that of a liquid sample observed in acetonitrile (1082, 1059, 955, 889, 811, and 733 cm^{-1}); this showed that the molecular structure of $[(n\text{-C}_4\text{H}_9)_4\text{N}]_{4.25}\text{H}_{2.75}[\alpha\text{-PW}_{11}\text{MgO}_{40}] \cdot \text{H}_2\text{O} \cdot \text{CH}_3\text{CN}$ observed in a solid was the same as that in acetonitrile solution. In contrast, the spectral pattern of solid $\text{Cs}_{5.25}\text{H}_{1.75}[\alpha\text{-PW}_{11}\text{MgO}_{40}] \cdot 6\text{H}_2\text{O}$ was somewhat different from that in water (1079, 1056, 1017, 957, 898, 823, 779, and 724 cm^{-1}). Since a single line was observed in the ^{31}P NMR spectrum of $\text{Cs}_{5.25}\text{H}_{1.75}[\alpha\text{-PW}_{11}\text{MgO}_{40}] \cdot 6\text{H}_2\text{O}$ in D_2O at around 25 $^\circ\text{C}$, this change was not due to decomposition of the cesium salt in aqueous solution; however, water may have influenced the structure.

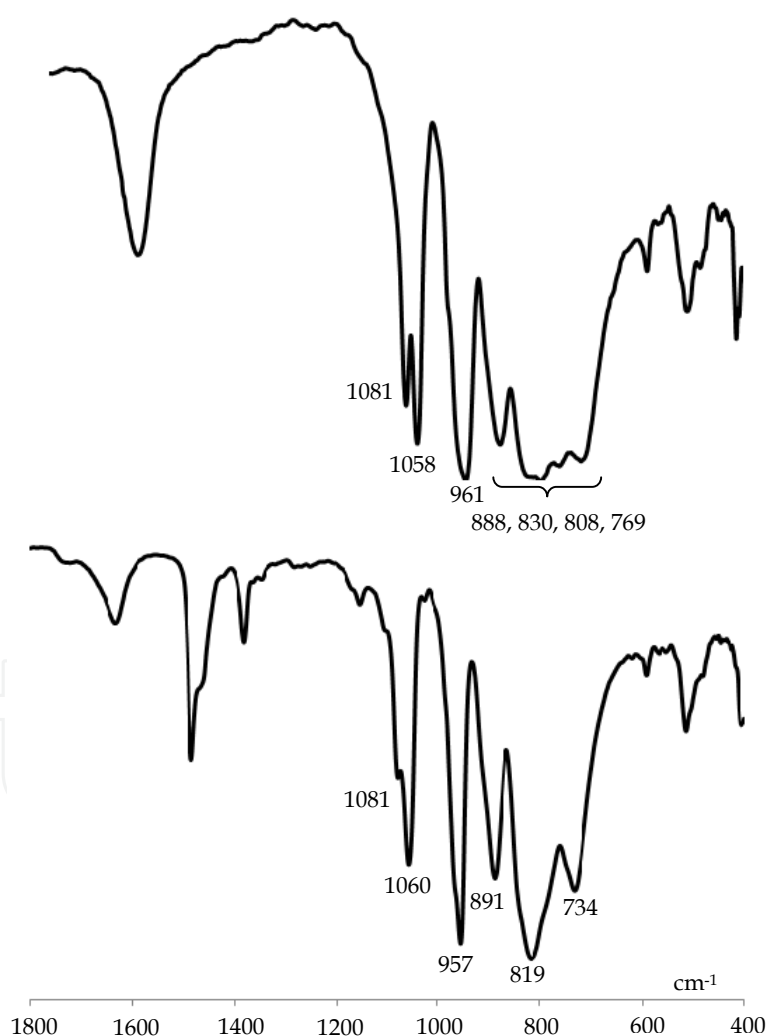


Figure 4. FT-IR spectra (as KBr disks) of $\text{Cs}_{5.25}\text{H}_{1.75}[\alpha\text{-PW}_{11}\text{MgO}_{40}] \cdot 6\text{H}_2\text{O}$ (top) and $[(n\text{-C}_4\text{H}_9)_4\text{N}]_{4.25}\text{H}_{2.75}[\alpha\text{-PW}_{11}\text{MgO}_{40}] \cdot \text{H}_2\text{O} \cdot \text{CH}_3\text{CN}$ (bottom) in the range of 1800 – 400 cm^{-1} .

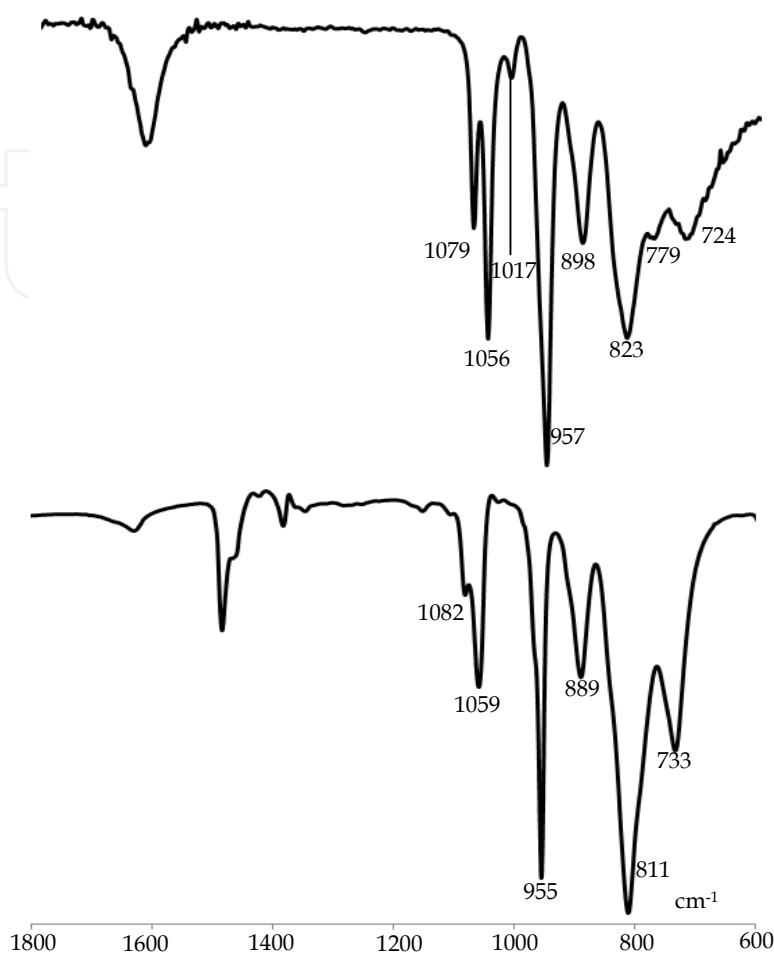


Figure 5. FT-IR spectra of $\text{Cs}_{5.25}\text{H}_{1.75}[\alpha\text{-PW}_{11}\text{MgO}_{40}] \cdot 6\text{H}_2\text{O}$ observed in water (top) and $[(n\text{-C}_4\text{H}_9)_4\text{N}]_{4.25}\text{H}_{2.75}[\alpha\text{-PW}_{11}\text{MgO}_{40}] \cdot \text{H}_2\text{O} \cdot \text{CH}_3\text{CN}$ observed in acetonitrile (bottom) in the range of 1800 – 600 cm^{-1} .

3.2. Syntheses and molecular structures of potassium and dimethylammonium salts of α -Dawson-type mono-magnesium-substituted polyoxotungstate $\text{K}_8\text{H}_2[\alpha_2\text{-P}_2\text{W}_{17}\text{MgO}_{62}] \cdot 15\text{H}_2\text{O}$ and $[(\text{CH}_3)_2\text{NH}_2]_{7.5}\text{H}_{2.5}[\alpha_2\text{-P}_2\text{W}_{17}\text{MgO}_{62}] \cdot 6\text{H}_2\text{O}$

The potassium salt of $[\alpha_2\text{-P}_2\text{W}_{17}\text{MgO}_{62}]^{10-}$ was formed by the direct reaction of magnesium bromide with $[\alpha_2\text{-P}_2\text{W}_{17}\text{O}_{61}]^{10-}$ (at a $\text{Mg}^{2+}/[\alpha_2\text{-P}_2\text{W}_{17}\text{O}_{61}]^{10-}$ molar ratio of ~ 3.0) in aqueous solution, followed by the addition of excess potassium chloride. Pure potassium salt was not obtained by the stoichiometric reaction of magnesium ions with $[\alpha_2\text{-P}_2\text{W}_{17}\text{O}_{61}]^{10-}$ in aqueous solution, as was observed for $\text{Cs}_{5.25}\text{H}_{1.75}[\alpha\text{-PW}_{11}\text{MgO}_{40}] \cdot 6\text{H}_2\text{O}$. In contrast, the dimethylammonium salt was formed via a stoichiometric reaction of magnesium nitrate with $[\alpha_2\text{-P}_2\text{W}_{17}\text{O}_{61}]^{10-}$ in aqueous solution, followed by the addition of excess dimethylammonium chloride. Crystallization was performed by vapor diffusion from water/ethanol at around 25 $^\circ\text{C}$.

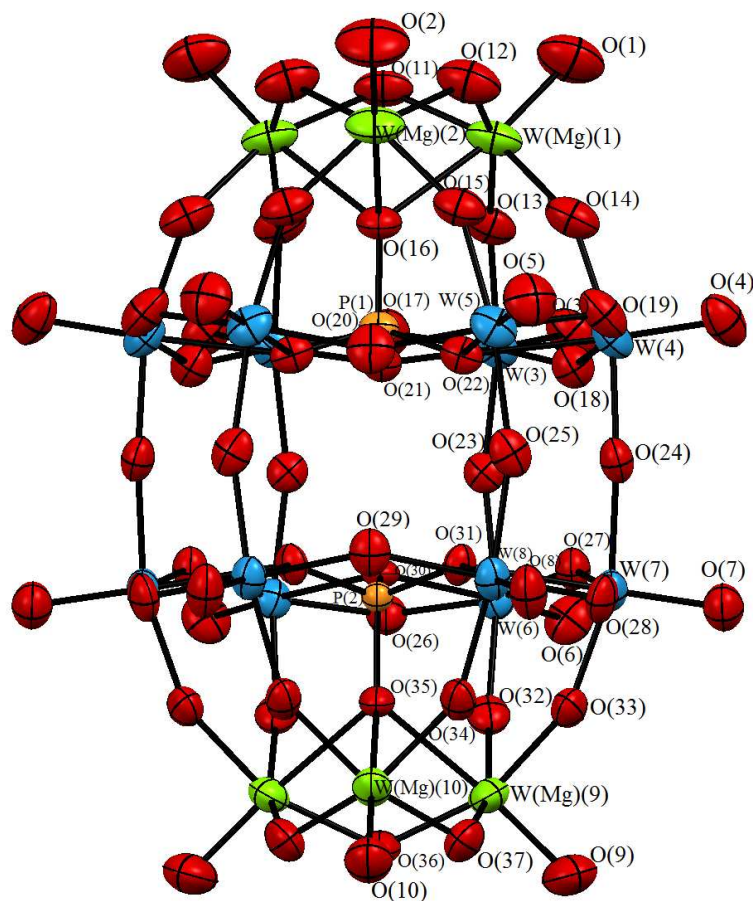


Figure 6. Molecular structure (ORTEP drawing) of $[(\text{CH}_3)_2\text{NH}_2]_{7.5}\text{H}_{2.5}[\alpha_2\text{-P}_2\text{W}_{17}\text{MgO}_{62}]\cdot 6\text{H}_2\text{O}$. One magnesium atom was disordered over six tungsten atoms at the B-sites (i.e., cap units) in $[\alpha_2\text{-P}_2\text{W}_{17}\text{MgO}_{62}]^{10-}$. The occupancies for the magnesium and tungsten sites were fixed at 1/6 and 5/6 throughout the refinement; however, the populations of these atoms differed.

The elemental analysis results for H, K, Mg, P, and W were in good agreement with the calculated values for $\text{K}_8\text{H}_2[\alpha_2\text{-P}_2\text{W}_{17}\text{MgO}_{62}]\cdot \text{H}_2\text{O}$. N analysis revealed no contamination of nitrate ions from $\text{Mg}(\text{NO}_3)_2$. The weight loss observed during drying before the analysis was 5.30% for $\text{K}_8\text{H}_2[\alpha_2\text{-P}_2\text{W}_{17}\text{MgO}_{62}]\cdot 15\text{H}_2\text{O}$; this corresponded to 14 weakly solvated or adsorbed water molecules. TG/DTA data also showed a weight loss of 5.62% in the temperature range of 25 to 500 °C, which corresponded to 15 water molecules. For the dimethylammonium salt, the C, H, N, P, Mg, and W elemental analysis results were in good agreement with the calculated values for $[(\text{CH}_3)_2\text{NH}_2]_{7.5}\text{H}_{2.5}[\alpha_2\text{-P}_2\text{W}_{17}\text{MgO}_{62}]\cdot 3\text{H}_2\text{O}$. The K analysis revealed no contamination of potassium ions from $\text{K}_{10}[\alpha_2\text{-P}_2\text{W}_{17}\text{O}_{61}]\cdot 14\text{H}_2\text{O}$. The weight loss observed during drying before the analysis was 1.30% for $[(\text{CH}_3)_2\text{NH}_2]_{7.5}\text{H}_{2.5}[\alpha_2\text{-P}_2\text{W}_{17}\text{MgO}_{62}]\cdot 6\text{H}_2\text{O}$; this corresponded to three weakly solvated molecules. TG/DTA data showed weight losses of 2.33 and 7.42% observed in the temperature ranges of 25 to 200 °C and 200 to 500 °C, respectively; these values corresponded to six water molecules and 7.5 $[(\text{CH}_3)_2\text{NH}_2]^+$ ions, respectively.

[(CH ₃) ₂ NH ₂] _{7.5} H _{2.5} [α ₂ -P ₂ W ₁₇ MgO ₆₂]·6H ₂ O	
belt units (W(3) – W(8))	
W-O _a	2.338 – 2.374 (2.359)
W-O _c	1.874 – 1.962 (1.908)
W-O _e	1.904 – 1.935 (1.924)
W-O _t	1.698 – 1.733 (1.717)
cap units (W(Mg) (1), W(Mg)(2), W(Mg)(9), W(Mg)(10))	
W(Mg)-O _a	2.348 – 2.393 (2.369)
W(Mg)-O _c	1.909 – 1.966 (1.934)
W(Mg)-O _e	1.910 – 1.948 (1.930)
W(Mg)-O _t	1.73 – 1.788 (1.760)
P-O	1.505 – 1.584 (1.538)

Table 4. Ranges and mean bond distances (Å) of [(CH₃)₂NH₂]_{7.5}H_{2.5}[α₂-P₂W₁₇MgO₆₂]·6H₂O. O_a: oxygen atoms belonging to the central PO₄ tetrahedron; O_c: bridging oxygen atoms between corner-sharing MO₆ (M = Mg and W) octahedra; O_e: bridging oxygen atoms between edge-sharing MO₆ octahedra (M = Mg and W); and O_t: terminal oxygen atoms. Mean values are provided in parentheses.

The molecular structure of [(CH₃)₂NH₂]_{7.5}H_{2.5}[α₂-P₂W₁₇MgO₆₂]·6H₂O determined by X-ray crystallography is shown in Fig. 6. This molecular structure was identical to that of monomeric α-Dawson-type polyoxotungstate [α-P₂W₁₈O₆₂]⁶⁻ [23], which was constructed from cap (W(Mg) (1, 2, 9, 10)) and belt (W(3 – 8)) units. The bond lengths are summarized in Table 4. Because of the high symmetry of the space group, the six tungsten(VI) atoms at the two cap units were disordered and the partial structure around the magnesium site in [(CH₃)₂NH₂]_{7.5}H_{2.5}[α₂-P₂W₁₇MgO₆₂]·6H₂O was not identified by X-ray crystallography, as was observed for Cs_{5.25}H_{1.75}[α-PW₁₁MgO₄₀]·6H₂O and [(n-C₄H₉)₄N]_{4.25}H_{2.75}[α-PW₁₁MgO₄₀]·H₂O·CH₃CN; however, the W(Mg)–O_t bond lengths in the cap units (average 1.760 Å) were remarkably longer than those of W–O_t in the belt units (average 1.717 Å) and [α₂-P₂W₁₇O₆₁]¹⁰⁻ (~1.7 Å) [24]. Although it was difficult to discuss that the W(Mg)–O_t lengths of Cs_{5.25}H_{1.75}[α-PW₁₁MgO₄₀]·6H₂O and [(n-C₄H₉)₄N]_{4.25}H_{2.75}[α-PW₁₁MgO₄₀]·H₂O·CH₃CN were longer than those of [CH₃NH₃]₃[PW₁₂O₄₀]·2H₂O (1.6951 Å), [(CH₃)₂NH₂]₃[PW₁₂O₄₀] (1.7026 Å), and [(CH₃)₃NH]₃[PW₁₂O₄₀] (1.6933 Å) [19], the DFT calculation results for [α-PW₁₁{Mg(OH)}O₃₉]⁶⁻ and [α-PW₁₁{Mg(OH₂)}O₃₉]⁵⁻ showed that the Mg–OH₂ bond distance in [α-PW₁₁{Mg(OH₂)}O₃₉]⁵⁻ (2.12343 Å) was longer than that of Mg–OH in [α-PW₁₁{Mg(OH)}O₃₉]⁶⁻ (1.93732 Å) (Table 2). For the other magnesium compounds, the Mg–OH₂ bond lengths in [Mg(TDC)(H₂O)₂] (TDC = 2,5-tiophenedicarboxylate) (2.080 Å) [25] and Mg(3,5-PDC)(H₂O)₂ (PDC = pyridinedicarboxylate) (2.04 Å) [26] were longer than that of Mg–OH in [2MgSO₄·Mg(OH)₂] (2.025 Å) [27]. These results suggested that a water molecule was coordinated to the mono-magnesium-substituted site in [(CH₃)₂NH₂]_{7.5}H_{2.5}[α₂-P₂W₁₇MgO₆₂]·6H₂O.

The ^{31}P NMR spectrum of $\text{K}_8\text{H}_2[\alpha_2\text{-P}_2\text{W}_{17}\text{MgO}_{62}]\cdot 15\text{H}_2\text{O}$ in D_2O showed signals at -7.8 and -13.8 ppm, which were the same as those of $[(\text{CH}_3)_2\text{NH}_2]_{7.5}\text{H}_{2.5}[\alpha_2\text{-P}_2\text{W}_{17}\text{MgO}_{62}]\cdot 6\text{H}_2\text{O}$ (-7.7 and -13.7 ppm); this was also confirmed by the two-line spectrum observed for a mixture of the potassium and dimethylammonium salts in D_2O . These signals were different from those of $\text{K}_{10}[\alpha_2\text{-P}_2\text{W}_{17}\text{O}_{61}]\cdot 14\text{H}_2\text{O}$ ($\delta -6.8$ and -13.9), suggesting that a magnesium ion was coordinated to the vacant site of $[\alpha_2\text{-P}_2\text{W}_{17}\text{O}_{61}]^{10-}$. The ^{183}W NMR spectrum of $\text{K}_8\text{H}_2[\alpha_2\text{-P}_2\text{W}_{17}\text{MgO}_{62}]\cdot 15\text{H}_2\text{O}$ in $2.0\text{ mM Mg}(\text{NO}_3)_2\text{-D}_2\text{O}$ showed nine signals at -57.04 , -80.87 , -131.47 , -176.59 , -181.67 , -201.40 , -207.65 , -208.63 , and -230.51 , as shown in Fig. 7. These signals were also different from those of $\text{K}_{10}[\alpha_2\text{-P}_2\text{W}_{17}\text{O}_{61}]\cdot 14\text{H}_2\text{O}$ ($\delta -117.1$, -140.4 , -151.7 , -181.0 , -183.1 , -218.1 , -220.5 , -224.0 , and -242.6) observed in D_2O [28]. These results also supported that a magnesium ion was coordinated to the vacant site of $[\alpha_2\text{-P}_2\text{W}_{17}\text{O}_{61}]^{10-}$, resulting in an overall C_s symmetry.

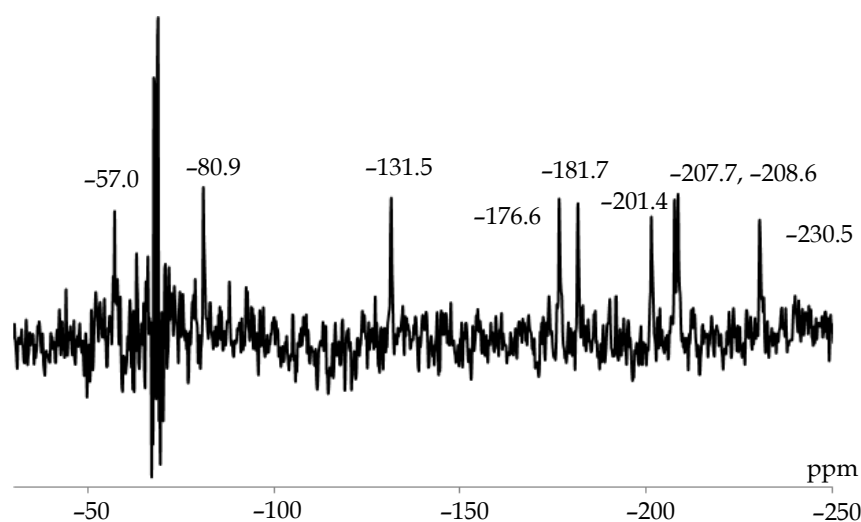


Figure 7. NMR spectrum of $\text{K}_8\text{H}_2[\alpha_2\text{-P}_2\text{W}_{17}\text{MgO}_{62}]\cdot 15\text{H}_2\text{O}$ in $2.0\text{ mM Mg}(\text{NO}_3)_2\text{-D}_2\text{O}$.

The FT-IR spectra of $\text{K}_8\text{H}_2[\alpha_2\text{-P}_2\text{W}_{17}\text{MgO}_{62}]\cdot 15\text{H}_2\text{O}$ and $[(\text{CH}_3)_2\text{NH}_2]_{7.5}\text{H}_{2.5}[\alpha_2\text{-P}_2\text{W}_{17}\text{MgO}_{62}]\cdot 6\text{H}_2\text{O}$ measured as KBr disks are shown in Fig. 8. The potassium and dimethylammonium salts showed bands at 1084 , 1063 , 1015 , 945 , 920 , 892 , 823 , 786 , and 736 cm^{-1} and 1087 , 1065 , 1018 , 948 , 919 , 891 , 805 , 777 , and 717 cm^{-1} , respectively. These bands were different from those of $\text{K}_{10}[\alpha_2\text{-P}_2\text{W}_{17}\text{O}_{61}]\cdot 14\text{H}_2\text{O}$ (1084 , 1051 , 1016 , 940 , 918 , 887 , 811 , 740 , and 601 cm^{-1}), which also supported that a magnesium atom was coordinated in the vacant site of $[\alpha_2\text{-P}_2\text{W}_{17}\text{O}_{61}]^{10-}$. The spectral pattern of solid $[(\text{CH}_3)_2\text{NH}_2]_{7.5}\text{H}_{2.5}[\alpha_2\text{-P}_2\text{W}_{17}\text{MgO}_{62}]\cdot 6\text{H}_2\text{O}$ was quite similar to that in water (1086 , 1065 , 1020 , 945 , 913 , 808 , 790 , and 723 cm^{-1}); this suggested that the molecular structure of $[(\text{CH}_3)_2\text{NH}_2]_{7.5}\text{H}_{2.5}[\alpha_2\text{-P}_2\text{W}_{17}\text{MgO}_{62}]\cdot 6\text{H}_2\text{O}$ observed in a solid was maintained in an aqueous solution. In addition, the FT-IR spectrum of $[(\text{CH}_3)_2\text{NH}_2]_{7.5}\text{H}_{2.5}[\alpha_2\text{-P}_2\text{W}_{17}\text{MgO}_{62}]\cdot 6\text{H}_2\text{O}$ observed in water was the same as that of a liquid sample of $\text{K}_8\text{H}_2[\alpha_2\text{-P}_2\text{W}_{17}\text{MgO}_{62}]\cdot 15\text{H}_2\text{O}$ (1086 , 1064 , 1015 , 946 , 914 , 811 , 788 , and 724 cm^{-1}). These results showed that the molecular structure of potassium salt was the same as that of the dimethylammonium salt, as suggested by the ^{31}P NMR spectra of the salts in D_2O .

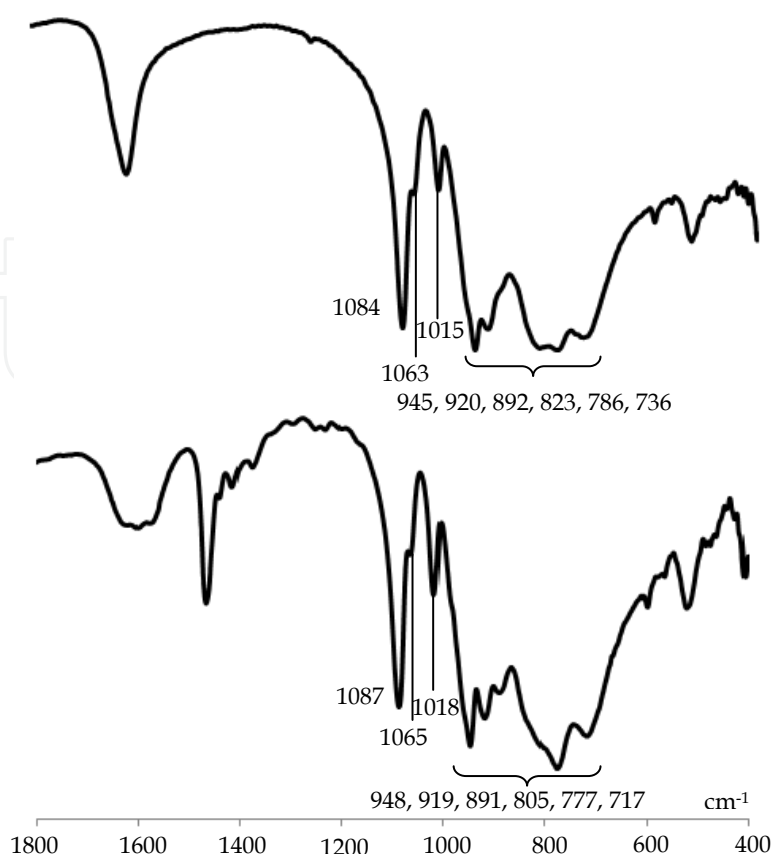


Figure 8. FTIR spectra (as KBr disks) of $\text{K}_8\text{H}_2[\alpha_2\text{-P}_2\text{W}_{17}\text{MgO}_{62}]\cdot 15\text{H}_2\text{O}$ (Top) and $[(\text{CH}_3)_2\text{NH}_2]_{7.5}\text{H}_{2.5}[\alpha_2\text{-P}_2\text{W}_{17}\text{MgO}_{62}]\cdot 6\text{H}_2\text{O}$ (bottom) in the range of 1800 – 400 cm^{-1} .

4. Conclusion

In this study, we synthesized α -Keggin-type mono-magnesium-substituted polyoxotungstate $\text{Cs}_{5.25}\text{H}_{1.75}[\alpha\text{-PW}_{11}\text{MgO}_{40}]\cdot 6\text{H}_2\text{O}$ and $[(n\text{-C}_4\text{H}_9)_4\text{N}]_{4.25}\text{H}_{2.75}[\alpha\text{-PW}_{11}\text{MgO}_{40}]\cdot \text{H}_2\text{O}\cdot \text{CH}_3\text{CN}$, and α -Dawson-type mono-magnesium-substituted polyoxotungstate $\text{K}_8\text{H}_2[\alpha_2\text{-P}_2\text{W}_{17}\text{MgO}_{62}]\cdot 15\text{H}_2\text{O}$ and $[(\text{CH}_3)_2\text{NH}_2]_{7.5}\text{H}_{2.5}[\alpha_2\text{-P}_2\text{W}_{17}\text{MgO}_{62}]\cdot 6\text{H}_2\text{O}$ by reacting magnesium ions with monolacunary α -Keggin and α -Dawson-type phosphotungstates. The compounds were characterized by X-ray crystallography, elemental analysis, thermogravimetric/differential thermal analysis, Fourier-transform infrared spectra, and solution ^{31}P and ^{183}W nuclear magnetic resonance spectroscopy. The single-crystal X-ray structure analyses of $\text{Cs}_{5.25}\text{H}_{1.75}[\alpha\text{-PW}_{11}\text{MgO}_{40}]\cdot 6\text{H}_2\text{O}$, $[(n\text{-C}_4\text{H}_9)_4\text{N}]_{4.25}\text{H}_{2.75}[\alpha\text{-PW}_{11}\text{MgO}_{40}]\cdot \text{H}_2\text{O}\cdot \text{CH}_3\text{CN}$, and $[(\text{CH}_3)_2\text{NH}_2]_{7.5}\text{H}_{2.5}[\alpha_2\text{-P}_2\text{W}_{17}\text{MgO}_{62}]\cdot 6\text{H}_2\text{O}$ revealed monomeric, α -Keggin, and α -Dawson structures, respectively; the mono-magnesium-substituted sites could not be identified because of the high symmetry of the products. However, the bonding modes (i.e., bond lengths and bond angles) suggested that a hydroxyl group and/or water molecule were coordinated to the mono-magnesium-substituted site in $[\alpha\text{-PW}_{11}\text{MgO}_{40}]^{7-}$ and $[\alpha_2\text{-P}_2\text{W}_{17}\text{MgO}_{62}]^{10-}$. The DFT and zero-point energy calculation results also suggested that the molecular structures of $[\alpha\text{-}$

$\text{PW}_{11}\{\text{Mg}(\text{OH})\}\text{O}_{39}]^{6-}$ and $[\alpha\text{-PW}_{11}\{\text{Mg}(\text{OH}_2)\}\text{O}_{39}]^{5-}$ were significantly influenced by coordination of a hydroxyl group and water molecule to the magnesium site, and $[\alpha\text{-PW}_{11}\{\text{Mg}(\text{OH}_2)\}\text{O}_{39}]^{5-}$ was more stable than $[\alpha\text{-PW}_{11}\{\text{Mg}(\text{OH})\}\text{O}_{39}]^{6-}$.

Acknowledgements

This work was supported by a Grant-in-Aid for Scientific Research of the Ministry of Education, Culture, Sports, Science and Technology, Japan.

Author details

Chika Nozaki Kato^{1*}, Nami Ukai¹, Daisuke Miyamae¹, Shunya Arata¹, Toshifumi Kashiwagi¹, Masaru Nagami¹, Toshiya Mori¹, Yusuke Kataoka², Yasutaka Kitagawa³ and Hidemitsu Uno⁴

*Address all correspondence to: sckatou@ipc.shizuoka.ac.jp

1 Shizuoka University, Japan

2 Shimane University, Japan

3 Osaka University, Japan

4 Ehime University, Japan

References

- [1] Pope MT. Heteropoly and Isopoly Oxometalates. Berlin: Springer-Verlag; 1983.
- [2] Pope MT, Müller A. Polyoxometalate Chemistry. An Old Field with New Dimensions in Several Disciplines. *Angewandte Chemie International Edition in English* 1991; 30 (1) 34–48.
- [3] Pope MT, Müller A., editors. Polyoxometalates: From Platonic Solids to Anti-Retroviral Activity. Dordrecht: Kluwer Academic Publishers; 1994.
- [4] Cotton, FA, Wilkinson G. Advanced Inorganic Chemistry, Fifth Edition. New York: John Wiley & Sons; 1988.
- [5] Ono Y, Hattori H. Solid Base Catalysis. Berlin: Springer-Verlag and Tokyo Institute of Technology Press; 2011.

- [6] Günter JR, Bensch W. Two New Trigonal Magnesium Heteropolytungstates: Crystal Structures, Topotactic Relations, and Thermal Dehydration. *Journal of Solid State Chemistry* 1987; 69 (2) 202–214.
- [7] Günter JR, Schmalte HW, Dubler E. Crystal Structure and Properties of A New Magnesium Heteropoly-tungstate, $\text{Mg}_7(\text{MgW}_{12}\text{O}_{42})(\text{OH})_4(\text{H}_2\text{O})_8$, and The Isostructural Compounds of Manganese, Iron, Cobalt, and Nickel. *Solid State Ionics* 1990; 43 85–92.
- [8] Contant R. Relation between Tungstophosphates Related to the Phosphorus Tungsten Oxide Anion ($\text{PW}_{12}\text{O}_{40}^{3-}$). Synthesis and Properties of a New Lacunary Potassium Polyoxotungstophosphate ($\text{K}_{10}\text{P}_2\text{W}_{20}\text{O}_{70}\cdot 24\text{H}_2\text{O}$). *Canadian Journal of Chemistry* 1987; 65 (3) 568–573.
- [9] Lyon DK, Miller WK, Novet T, Domaille PJ, Evitt E, Johnson DC, Finke RG. Highly Oxidation Resistant Inorganic-Porphyrin Analog Polyoxometalate Oxidation Catalysts. 1. The Synthesis and Characterization of Aqueous-Soluble Potassium Salts of $\alpha_2\text{-P}_2\text{W}_{17}\text{O}_{61}(\text{M}^{n+}\cdot\text{OH}_2)^{(n-10)}$ and Organic Solvent Soluble Tetra-n-butylammonium Salts of $\alpha_2\text{-P}_2\text{W}_{17}\text{O}_{61}(\text{M}^{n+}\cdot\text{Br})^{(n-11)}$ ($\text{M} = \text{Mn}^{3+}, \text{Fe}^{3+}, \text{Co}^{2+}, \text{Ni}^{2+}, \text{Cu}^{2+}$). *Journal of the American Chemical Society* 1991; 113 (19) 7209–7221.
- [10] Burla MC, Caliendo R, Camalli M, Carrozzini B, Cascarano GL, De Caro L, Giacovazzo C, Polidori G, Spagna R. *SIR2004*: An Improved Tool for Crystal Structure Determination and Refinement. *Journal of Applied Crystallography* 2005; 38 (2) 381–388.
- [11] Sheldrick GM. A Short History of SHELX. *Acta Crystallographica Section A* 2008; A64 (1) 112–122.
- [12] Spek, AL. Structure Validation in Chemical Crystallography. *Acta Crystallographica Section D* 2009; D65 (2) 148–155.
- [13] Nomiya K, Takahashi M, Ohsawa K, Widegren JA. Synthesis and Characterization of Tri-titanium(IV)-1,2,3-substituted α -Keggin Polyoxotungstates with Heteroatoms P and Si. Crystal Structure of the Dimeric, Ti-O-Ti Bridged Anhydride Form $\text{K}_{10}\text{H}_2[\alpha, \alpha\text{-P}_2\text{W}_{18}\text{Ti}_6\text{O}_{77}]\cdot 17\text{H}_2\text{O}$ and Confirmation of Dimeric Forms in Aqueous Solution by Ultracentrifugation Molecular Weight Measurements. *Journal of the Chemical Society Dalton Transactions* 2001; 19 2872–2878.
- [14] Nomiya K, Takahashi M, Widegren JA, Aizawa T, Sakai Y, Kasuga NC. Synthesis and pH-Variable Ultracentrifugation Molecular Weight Measurements of the Dimeric, Ti-O-Ti Bridged Anhydride Form of a Novel Di-Ti^{IV}-1,2-substituted α -Keggin Polyoxotungstate. Molecular Structure of the $[(\alpha\text{-1,2-PW}_{10}\text{Ti}_2\text{O}_{39})_2]^{10-}$ Polyoxoanion. *Journal of the Chemical Society Dalton Transactions* 2002; 19 3679–3685.
- [15] Weakley TJR, Finke RG. Single-crystal X-Ray Structures of the Polyoxotungstate Salts $\text{K}_{8.3}\text{Na}_{1.7}[\text{Cu}_4(\text{H}_2\text{O})_2(\text{PW}_9\text{O}_{34})_2]\cdot 24\text{H}_2\text{O}$ and $\text{Na}_{14}\text{Cu}[\text{Cu}_4(\text{H}_2\text{O})_2(\text{P}_2\text{W}_{15}\text{O}_{56})_2]\cdot 53\text{H}_2\text{O}$. *Inorganic Chemistry* 1990; 29 (6) 1235–1241.

- [16] Lin Y, Weakley TJR, Rapko B, Finke RG. Polyoxoanions Derived from Tungstosilicate ($A\text{-}\beta\text{-SiW}_9\text{O}_{34}^{10-}$): Synthesis, Single-crystal Structural Determination, and Solution Structural Characterization by Tungsten-183 NMR and IR of Titanotungstosilicate ($A\text{-}\beta\text{-Si}_2\text{W}_{18}\text{Ti}_6\text{O}_{77}^{14-}$). *Inorganic Chemistry* 1993; 32 (23) 5095–5101.
- [17] Frisch MJ, Trucks GW, Schlegel HB, Scuseria GE, Robb MA, Cheeseman JR, Scalmani G, Barone V, Mennucci B, Petersson GA, Nakatsuji H, Caricato M, Li X, Hratchian HP, Izmaylov AF, Bloino J, Zheng G, Sonnenberg JL, Hada M, Ehara M, Toyota K, Fukuda R, Hasegawa J, Ishida M, Nakajima T, Honda Y, Kitao O, Nakai H, Vreven T, Montgomery JA, Peralta JE, Ogliaro F, Bearpark M, Heyd JJ, Brothers E, Kudin KN, Staroverov VN, Kobayashi R, Normand J, Raghavachari K, Rendell A, Burant JC, Iyengar SS, Tomasi J, Cossi M, Rega N, Millam JM, Klene M, Knox JE, Cross JB, Bakken V, Adamo C, Jaramillo J, Gomperts R, Stratmann RE, Yazyev O, Austin AJ, Cammi R, Pomelli C, Ochterski JW, Martin RL, Morokuma K, Zakrzewski VG, Voth GA, Salvador P, Dannenberg JJ, Dapprich S, Daniels AD, Farkas Ö, Foresman JB, Ortiz JV, Cioslowski J, Fox DJ. Gaussian 09, Revision B, 01, Wallingford CT: Gaussian, Inc.; 2009.
- [18] Neiwert WA, Cowan JJ, Hardcastle KI, Hill CL, Weinstock IA. Stability and Structure in α - and β -Keggin Heteropolytungstates, $[X^{n+}W_{12}O_{40}]^{(8-n)-}$, $X = p\text{-Block Cation}$. *Inorganic Chemistry* 2002; 41 (26) 6950–6952.
- [19] Busbongthong S, Ozeki T. Structural Relationships among Methyl-, Dimethyl-, and Trimethylammonium Phosphododecatungstates. *Bulletin of Chemical Society in Japan* 2009; 82 (11) 1393–1397.
- [20] Kato CN, Makino Y, Yamasaki M, Kataoka U, Kitagawa Y, Okumura M. Synthesis and X-Ray Crystal Structure of α -Keggin-type Aluminum-substituted Polyoxotungstate. *Advances in Crystallization processes*, Rijeka: InTech; 2012.
- [21] Rocchiccioli-Deltcheff C, Fournier M, Franck R, Thouvenot R. Vibrational Investigations of Polyoxometalates. 2. Evidence for Anion-Anion Interactions in Molybdenum(VI) and Tungsten(VI) Compounds Related to the Keggin Structure. *Inorganic Chemistry* 1983; 22 207–216.
- [22] Thouvenot R, Fournier M, Franck R, Rocchiccioli-Deltcheff C. Vibrational Investigations of Polyoxometalates. 3. Isomerism in Molybdenum(VI) and Tungsten(VI) Compounds Related to the Keggin Structure. *Inorganic Chemistry* 1984; 23 (5) 598–605.
- [23] Dawson B. The Structure of the 9(18)-Heteropoly Anion in Potassium 9(18)-Tungstophosphate, $K_6(P_2W_{18}O_{62}) \cdot 14H_2O$. *Acta Crystallographica* 1953; 6 113–126.
- [24] Sakai Y, Shinohara A, Hayashi K, Nomiya K. Synthesis and Characterization of Two Novel, Mono-lacunary Dawson Polyoxometalate-based, Water-soluble Organometallic Ruthenium(II) Complexes: Molecular Structure of $[(C_6H_6)Ru(H_2O)](\alpha_2\text{-}P_2W_{17}O_{61})]^{8-}$. *European Journal of Inorganic Chemistry* 2006; 163 – 171.

- [25] Calderone PJ, Banerjee D, Santulli AC, Wong SS, Parise JB. Synthesis, Characterization, and Luminescence Properties of Magnesium Coordination Networks using a Thiophene-based Linker. *Inorganica Chimica Acta* 2011; 378 (1) 109–114.
- [26] Banerjee D, Finkelstein J, Smirnov A, Forster PM, Borkowski LA, Teat SJ, Parise JB. Synthesis and Structural Characterization of Magnesium Based Coordination Networks in Different Solvents. *Crystal Growth & Design* 2011; 11 (6) 2572–2579.
- [27] Fleet ME, Knipe SW. Structure of Magnesium Hydroxide Sulfate $[2\text{MgSO}_4 \cdot \text{Mg}(\text{OH})_2]$ and Solid Solution in Magnesium Hydroxide Sulfate Hydrate and Caminite. *Acta Crystallographica* 1997; B53 (3) 358–363.
- [28] Kato CN, Shinohara A, Hayashi K, Nomiya K. Syntheses and X-ray Crystal Structures of Zirconium(IV) and Hafnium(IV) Complexes Containing Monovacant Wells-Dawson and Keggin Polyoxotungstates. *Inorganic Chemistry* 2006; 45 (20) 8108–8119.

IntechOpen

